

# OPTICAL FIBER BASED BEAM LOSS MONITOR FOR THE BINP E-E+ INJECTION COMPLEX

Yu.I. Maltseva\*, V.G. Prisekin,  
 Budker Institute of Nuclear Physics SB RAS, Novosibirsk, Russian Federation

## Abstract

A distributed optical fiber based beam loss monitor has been implemented for the Budker INP Injection Complex designed to accelerate and store electron and positron beams up to 500 MeV. The principle of the device operation consists in detecting the Cherenkov radiation generated in an optical fiber by relativistic charged particles produced in an electromagnetic shower when beam hits the accelerator vacuum chamber wall. Single optical fiber section can cover the entire accelerator instead of using a large number of local beam loss monitors. Timing of optical signal gives the location of the beam losses along the beamline. In this paper summary of the monitor application at the BINP Injection Complex is given. Methods to improve monitor spatial resolution are discussed.

## INTRODUCTION

Since 2016 Injection Complex [1–3] supplies two BINP colliders with high energy electron and positron beams (up to 500 MeV). In order to control beam losses along beamline during the Complex operation we proposed to use a distributed beam loss monitor based on the Cherenkov effect in an optical fiber [4].

This type of beam loss monitor has been developed at several facilities such as FLASH (DESY), SPring-8 (RIKEN/JASRI), CLIC Test Facility (CERN) [5–7]. The monitor overview is given by T. Obina [8].

Compared with other distributed beam loss monitors such as long ionization chamber and scintillating fiber, optical fiber beam loss monitor (OFBLM) has the following advantages: fast response time (< 1 ns), near zero sensitivity to background signal (mainly gamma radiation) and synchrotron radiation, unlike scintillating fiber. Optical fiber is insensitive to magnetic field, but it is susceptible to radiation damage (except quartz fiber), which limits fiber lifetime. Another disadvantage of the OFBLM is its signal calibration.

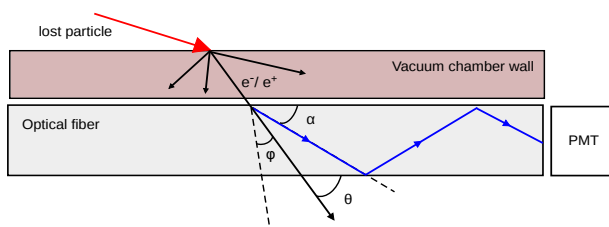


Figure 1: Scheme of beam loss monitor.

The basic idea behind the OFBLM is to detect a burst of the Cherenkov radiation (CR) generated in the optical

\* yu.i.maltseva@inp.nsk.su

fiber (OF) by means of relativistic particles created in electromagnetic shower after highly relativistic beam particles (electrons or positrons) hit the vacuum pipe. Some of the Cherenkov photons propagate in the fiber and can be detected by photomultiplier tube (PMT) (Fig. 1). For electromagnetic shower simulation G4beamline code [9] was used.

## CHERENKOV RADIATION GENERATION

To generate the CR the kinetic energy of charged particle propagating through a dielectric medium must satisfy the condition:  $E_k > E_0(n/\sqrt{n^2 - 1} - 1)$ , where  $E_0$  – particle rest energy,  $n$  – medium refractive index. According to our simulations, for the CR to be generated kinetic energy of lost particles hitting the vacuum pipe must be greater than 5 MeV for electron or positron beam. The CR is emitted in a cone around the moving charged particle with cone semi-angle,  $\cos \varphi = 1/(\beta n)$ . Since the average kinetic energy of the electron component of the shower is about 15 MeV, the CR photons are emitted with  $48^\circ$ .

The number of the CR photons generated by single electron or positron per unit radiation wavelength  $\lambda$  per unit path length  $x$  of the particle in a medium is given by:

$$\frac{d^2N}{d\lambda dx} = \frac{2\pi \sin^2 \varphi}{137\lambda^2} \quad (1)$$

According to eq. (1), the greater part of the CR photons is emitted in the ultraviolet (UV) range of the spectrum. For relativistic electron passing through the plastic OF ( $n = 1.49$ ) the number of the CR photons generated in UV-visible spectrum ( $300 \text{ nm} < \lambda < 700 \text{ nm}$ ) per mm is equal to 50.

## CHERENKOV LIGHT PROPAGATION IN OPTICAL FIBER

### Main Principle

The emitted CR propagates in the OF by means of total internal reflection with angles  $\alpha \leq \alpha_{max} = \sin^{-1}(NA/n_c)$  relative to the fiber axis (see Fig. 1), where  $NA$  – OF numerical aperture,  $n_c$  – refractive index of the OF core. For plastic OF with typical values of  $NA = 0.47$  and  $n_c = 1.49$ ,  $\alpha \leq 18^\circ$ . For quartz one with  $NA = 0.22$  and  $n_c = 1.46$ ,  $\alpha \leq 9^\circ$ . Thus, the greater  $NA$ , the higher the number of propagating photons.

Neglecting attenuation effects, the portion of total CR photons to be transmitted in the fiber by guided rays is given by [10]:

$$P = \frac{1}{\pi} \cos^{-1} \left( \frac{\beta n_c \cos \alpha_{max} - \cos \theta}{\sin \theta \sqrt{\beta^2 n_c^2 - 1}} \right) \quad (2)$$

where  $\theta$  – angle of the charged particle propagation relative to the fiber axis.

As one can see from eq. (2), the CR transmission efficiency depends on propagation angle of charged particle passing through the OF and fiber parameters. Secondary charged particles passing through OF with angles  $\theta \in [|\varphi - \alpha_{max}|, \varphi + \alpha_{max}]$  relative to the fiber axis generate the CR which is trapped in the OF and transmitted by guided rays. For plastic OF this value lies in range of 30°-66°, for quartz one: 38°-56°. According to our simulations for typical Injection Complex particle loss scenario, 10% and 5% of total generated light are able to exit plastic and quartz fiber end face, respectively.

Angular distributions of generated photons and photons transmitted by guided rays in plastic OF from the secondary e-/e+ passing through the OF when single electron hits the vacuum pipe, are shown in Fig. 2.

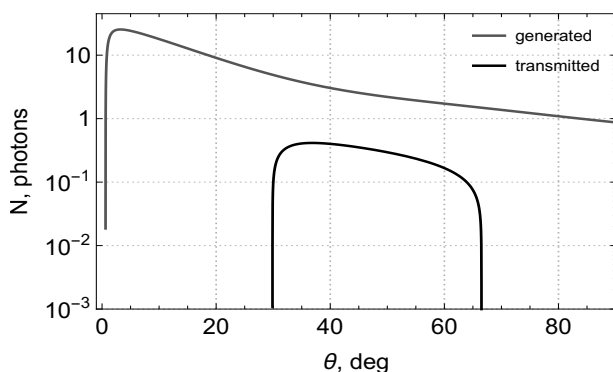


Figure 2: Angular distributions of generated photons (gray) and photons transmitted by guided rays in the OF (black). 500 MeV electron hits 2 mm steel vacuum pipe with 1° incident angle, plastic OF is placed at the loss point. Angular distribution of secondary e-/e+ passing through the OF is taken into account.

The photon yield from a wide transverse e-/e+ flow passing through the OF is  $\sim d^2$ , where  $d$  - fiber core diameter, and slightly depends on  $NA$ . In case of minor beam losses one should use the OF with large diameter for better photon yield to be able to detect losses. For singlemode OF with  $d \sim 10$   $\mu\text{m}$  the photon yield is  $10^4$  times lower than for the OF with 1 mm core diameter.

### Signal Attenuation

During propagation light signal undergoes attenuation. In the UV and visible parts of the spectrum signal attenuation is mostly caused by Rayleigh scattering, then signal output is  $\sim 1/\lambda^2 10^{-0.1aL\lambda^{-4}}$ , where  $a = 0.82$  and  $1.56$  for quartz and plastic fiber, respectively,  $L$  - fiber length. Neglecting cable losses, signal attenuation influence on the CR spectrum depending on the OF length is shown in Fig. 3.

Propagating through 10 m long plastic OF, the CR signal is decreased by 13%, 20 m – 25%, 50 m – 45%, 100 m – 65%. Moreover, the UV part of the spectrum is attenuated

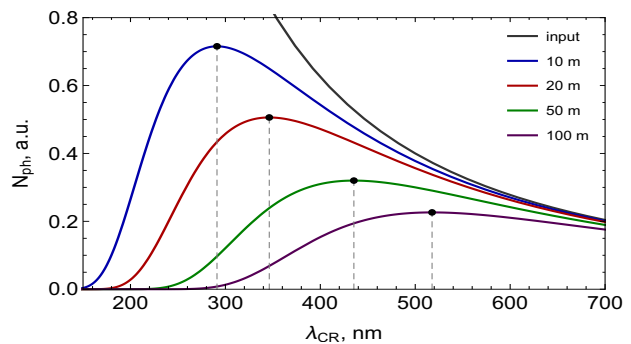


Figure 3: The input CR spectrum (gray) and output ones (colored) after signal propagating in 10 m, 20 m, 50 m, 100 m long plastic OF.

faster, thus, there is no reason to use long OF with operation wavelength range in the UV spectrum.

### Signal Dispersion

There are two main dispersion types in the fiber: modal and material. While transmitting signal through OF of length  $L$  each dispersion contribution to pulse broadening can be estimated for different fiber types as shown in Table 1.

Table 1: Estimated pulse lengthening due to dispersion for different fiber core materials and refractive index profiles.

core material	plastic		quartz	
$n$ profile	step	graded	step	graded
$t_{mod}/L$ , ns/m	0.25	0.007	0.055	0.0005
$t_{mat}/L$ , ns/m	0.08	0.08	0.05	0.05

As one can see from the table, for plastic step-index multimode fiber which was used in our tests modal dispersion contributes 5 times greater to the monitor spatial resolution than material one.

### Collimator

When it is required to minimize light pulse duration entering the PMT window, one may use a collimator attached to the fiber end face. In the simplest case, it is a hollow cylinder that absorbs light propagating with large angles relative to the fiber axis. Then, contribution of modal dispersion decreases as function of collimator length as:

$$t_{mod}/L \approx \frac{1}{cn_c} \frac{1}{1 + 4l_{coll}^2/d_{coll}^2} \quad (3)$$

where  $l_{coll}$ ,  $d_{coll}$  – collimator length and inner diameter.

Eq. (3) demonstrates 2 mm long collimator with inner diameter as fiber one is enough to reduce modal dispersion in the OF. Dependence of the monitor spatial resolution on length of the collimator attached to the end of the fiber was studied in our tests. For 10 m long plastic step-index multimode fiber collimator can improve monitor spatial resolution by 20 %.

## MONITOR SPATIAL RESOLUTION OPTIMIZATION

Monitor spatial resolution depends on light dispersion in OF, PMT and ADC time resolutions. To improve monitor spatial resolution graded-index multimode optical fiber, singlemode one or step-index multimode fiber along with collimator should be used as well as PMT and electronics with small time resolution ( $< 0.1$  ns). Micro-channel plate or silicon PMT is a good candidate. ADC with sampling rate of 1 GHz and bandwidth of 250 MHz is preferable.

PMT signal strength and FWHM of the signal as a function of the fiber length were also studied (Fig. 4). For the Injection Complex, taking into consideration strength of the light signal and its width, optimal length of the fiber was found to be about 20 m.

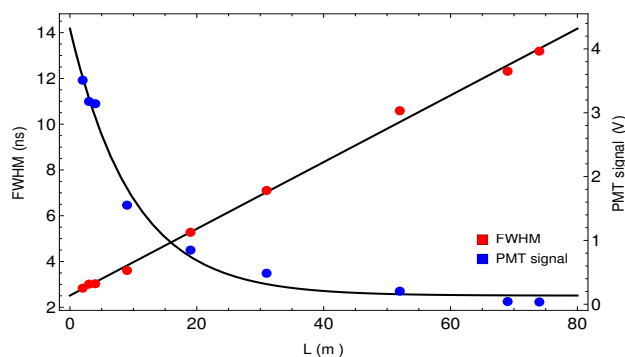


Figure 4: Measured PMT signal (blue) and FWHM of the signal (red) as a function of the fiber length.

The Cherenkov signal can be detected at either downstream or upstream ends of the fiber. In case of multiple losses originated from successive magnet elements 5 times better spatial discrimination between losses can be achieved by signal detection at the upstream end of the fiber compared with the downstream one. This is due to the fact that beam velocity  $\beta c$  is greater than speed of light in optical fiber  $c/n$ . Despite upstream signal sensitivity is 7 times lower than downstream one, the former is preferable.

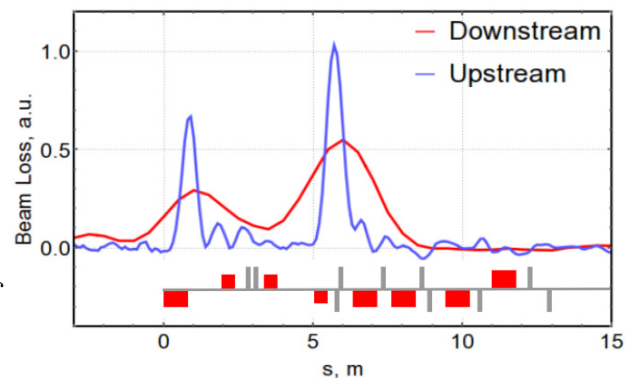


Figure 5: Downstream (red) and upstream (blue) losses of the electron beam at the storage ring extraction channel and first part of the K-500 transferline.

## EXPERIMENTAL RESULTS

The first tests of OFBLM operation at BINP Injection Complex were presented in article [4]. We use plastic step-index multimode fibers Avago Tech. HFBR-RUS500Z (1 mm core diameter,  $n_c = 1.492$  and  $NA = 0.47$ ), as CR detector we use micro-channel plate PMT (time res.  $< 0.1$  ns, 300-600 nm spectral sensitivity range). ADC with 1 GHz sampling rate and 250 MHz bandwidth was used.

The experimental results for electron loss monitoring at the downstream and upstream fiber ends are shown in Fig. 5. Although second loss is almost equidistant from both fiber ends, FWHM of the second signal approximately corresponds to 0.7 m and 3 m for the upstream and downstream measurements, respectively. Which leads to 4-5 times better spatial discrimination at the upstream fiber end.

## CONCLUSION

Optical fiber based beam loss monitor has been tested at the BINP Injection Complex. 0.7 m monitor spatial resolution for 15 m long optical fiber at the upstream end was obtained. Methods to optimize monitor spatial resolution are discussed. 0.5 m spatial resolution can be achieved by using 20 m long step-index multimode fiber along with collimator or graded-index multimode optical fiber or singlemode one and micro-channel plate PMT. To achieve better spatial discrimination between successive losses one should detect the light signal at the upstream end of the fiber.

## REFERENCES

- [1] D. Berkaev et al., "VEPP-5 Injection Complex: Two Colliders Operation Experience", Proc. of IPAC2017, Copenhagen, Denmark (2017) p. 2982
- [2] Yu. Maltseva et al., "VEPP-5 Injection Complex: New Possibilities for BINP Electron-Positron Colliders", Proc. of IPAC2018, Vancouver, BC, Canada (2018), p. 371
- [3] Yu.I. Maltseva et al., "VEPP-5 Injection Complex Performance Improvement for Two Collider Operation", this conference, paper TUZMH02
- [4] Maltseva Yu.I. et al., Physics-Uspekhi, Vol. 58, Issue 5, pp. 516-519 (2015)
- [5] F. Wulf, M. Korfer, "Beam Loss and Beam Profile Monitoring with Optical Fibers", Proc. DIPAC09, Basel, Switzerland (2009) 411
- [6] X.-M. Marechal et al., "Beam Based Development of a Fiber Beam Loss Monitor for the Spring-8/XFEL", Proc. DIPAC09, Basel, Switzerland (2009) 234
- [7] S. Mallows et al., "Fiber Based BLM System Research and Development at CERN", Proc. HB2012, Beijing, China (2012) 596
- [8] T. Obina, "Optical Fiber Based Loss Monitor for Electron Storage Ring", Proc. of IBIC2013, Oxford, UK (2013) 638
- [9] <http://www.muonsinternal.com/muons3/G4beamline>
- [10] Law S.H. et al., Applied Optics, Vol. 45, Issue 36, pp. 9151-9159 (2006)